Analyst

Pophyrin-loaded liposomes and graphenes oxide used for the membrane pore-forming protein assay and the inhibitor screening

Journal:	*Analyst*
Manuscript ID:	AN-COM-04-2015-000699.R1
Article Type:	Paper
Date Submitted by the Author:	25-May-2015
Complete List of Authors:	Liu, Zhongde; Southwest University, Long, Tengfei; Southwest University, College of Pharmaceutical Sciences Wu, Shuang; Southwest University, College of Pharmaceutical Sciences Li, Chong; Southwest University, College of Pharmaceutical Sciences

Journal Name

RSCPublishing

COMMUNICATION

Pophyrin-loaded liposomes and graphenes oxide used for the membrane pore-forming protein assay and the inhibitor screening

Zhongde Liu†, Tengfei Long, Shuang Wu and Chong Li†

Cite this: DOI: 10.1039/xoxxoooooox

Received ooth January 2012,
Accepted ooth January 2012

DOI: 10.1039/xoxxoooooox

www.rsc.org/

The interaction of planar aromatic molecules with the graphene oxide (GO) sheets is often marked by the fluorescence quenching of the former. Here, the α, β, γ, δ-tetrakis [4-(trimethylammoniumyl) phenyl] porphyrin (TAPP) molecules and the GO, corresponding to the energy donor and the acceptor respectively, are initially separated by encapsulating the TAPP molecules within the liposomes, to obstruct the formation of the self-assembled energy transfer-based quenching system. Upon disruption of the liposome membranes by the PLA_2 or the α-toxin, the encapsulated TAPP molecules are released and subsequently result in a significant fluorescence changes. Thus, a platform based on fluorescence signal for monitoring the activity of the membrane pore-forming protein with advantages of high sensitivity and commonality was established. Using this strategy, we can detect the PLA_2 and the α-toxin concentrations as low as 200 pM and 9.0 nM, respectively. Furthermore, by taking chlorpromazine and baicalin the examples, we use the assay to evaluate the prohibition effects on the PLA_2 and the α-toxin, and the IC_{50} value of chlorpromazine toward the PLA_2 (9.6 nM) and that of baicalin toward the α-toxin (289.2 nM) were found to be 12.0 ± 0.62 μM and 26.9 ± 2.6 μM, respectively.

Introduction

Phospholipase A_2 (PLA_2), an enzyme of the phospholipase superfamily, catalyzes the hydrolysis of phosphate ester bond in phospholipids to produce free fatty acids and lysolipids in a wide range of physiological processes[1]. Dysregulation of PLA_2 is a feature of many pathological conditions, and especially it can be a potential biomarker for diagnosing the degenerative disease atherosclerosis[2-3]. Alpha hemolysin, also named α-toxin, is one of the common toxins secreted by *Staphylococcus aureus* bacteria as a water-soluble protein monomer with a molecular weight of 33.2 kDa[4]. Upon binding to the membrane of susceptible host cells, the monomer oligomerizes to form a membrane-inserted heptamer, which causes the cell damage and death due to the leakage of ions, low molecular weight molecules mediated by the formed heptamers[4-5]. Therefore, flexible assays for both of them and inhibitor screening are highly desired for the development of efficient diagnostics, drug screening and detection of pathogens[6-7].

Although several artificial lipid analogues[8-9] or polypeptide encapsulated liposome[10] that undergo fluorometric or colometric changes upon hydrolysis have been created to determine the PLA_2 and can give high-resolution readings of PLA_2 activity, these systems suffer from the drawback that either the modified enzymatic substrate or the modified nanoparticles such as polypeptide immobilized gold nanoparticles are required. Moreover, it is worth mentioning that due to the demonstrated sensitivity of phospholipase to subtle changes in substrate chemistry and organization[10, 11-12], it would be preferable to have an assay based on unmodified and aggregated phospholipids organized into lipid bilayers. In addition, to the best of our knowledge, except for the phospholipase the studies on other species such as bacterial toxin-triggered liposome release and the efforts on the analytical application are far from comprehensive and mature.

The graphene, a two-dimensional nanomaterial consisting of sp^2-hybridized carbon atoms forming a one-atom thick honeycomb lattice, exhibits remarkable optoelectronic properties[13]. The interaction between the graphene oxide (GO) sheets and the planar aromatic molecules is often marked by the fluorescence quenching of the organic molecules and a few donor-acceptor-type nanohybrids have been reported, featuring the porphyrin derivatives as energy donor and the graphene sheets as energy acceptor to generate self-assembled energy transfer-based quenching system[13-18]. In addition, as mentioned above, it is the membrane pore-forming activity that both the PLA_2 and the α-toxin possess the common characteristics. Therefore in this contribution, as a proof-of-concept, a platform based on fluorescence signal for monitoring the activity of the membrane pore-forming protein and screening the corresponding inhibitors was established, by means of the combination of the α, β, γ, δ-tetrakis [4-(trimethylammoniumyl) phenyl] porphyrin (TAPP) loaded liposome and the GO sheets.

The rationale for this fluorometric assay is schematically illustrated in Scheme 1. Two key components, the TAPP molecules and the GO, corresponding to the energy donor and the acceptor respectively, are initially separated by encapsulating the TAPP molecules within the liposomes. However, once these liposomes see the PLA_2 or the α-toxin, they will form transmembrane pores in the liposome membranes, through which the encapsulated TAPP molecules are released and subsequently result in rapid and significant fluorescence changes due to the formation of the self-assembled quenching

system. Furthermore, by taking chlorpromazine and baicalin the examples, we use the assay to demonstrate the obvious positive prohibition effects on the PLA_2 and the α-toxin, respectively. Given its commonality and high sensitivity, this strategy provides a new alternative for a variety of other pore-forming species testing and the corresponding inhibitor screening.

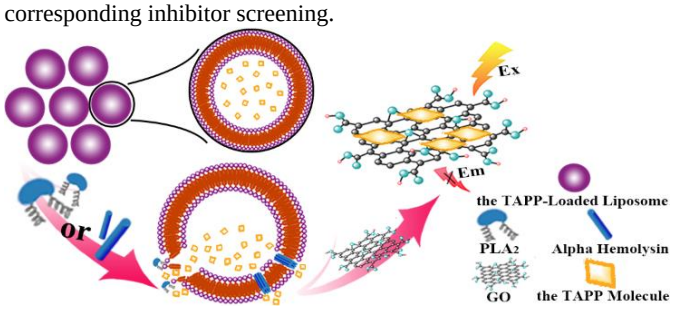

Scheme 1 Schematic illustration of the mechanism for fluorescent assay of phospholipase A_2 (PLA_2) and α-toxin.

Experimental section

Materials Soybean phosphatidylcholine (SPC) and cholesterol were supplied by AVT Pharmaceuticals, Ltd (Shanghai, China). Sephadex G-50, α, β, γ, δ-tetrakis- [4-(trimethylammoniumyl) phenyl] porphyrin (TAPP), phospholipases A_2 (PLA_2), alpha hemolysin (α-toxin) and baicalin were commercially obtained from Sigma-Aldrich. Natural graphite powder (325 mesh) was purchased from Nanjing XFNANO Materials Tech Co., Ltd. (Nanjing, PRC). All metal salts were of analytical grade and obtained from Beijing Chemical Reagent Co. Deionized water was used throughout the experiments, and all reagents described above were used as received without further purification.

Apparatus The fluorescence and the absorption spectra were recorded with a Hitachi F-7000 fluorescence spectrophotometer (Tokyo, Japan) and a Shimadzu UV-2450 spectrophotometer (Tokyo, Japan), respectively. The particle size of the as-prepared TAPP-loaded liposomes was determined using dynamic light scattering (Zetasizer Nano ZS, Malvern, UK) at 25 ℃. Transmission electron microscopy (JEM-1200EX) was used to characterize the morphology of TAPP-loaded liposomes using a negative staining method. Samples were pretreated with 2% phosphotungstic acid and then air-dried before measurement. The morphology of GO was observed on a Nanoscope Quadrex atom force microscope (Veeco, USA). A Fangzhong pHS-3C digital pH meter (Chengdu, China) was used to measure the pH values of the aqueous solutions and a vortex mixer QL-901 (Haimen, China) was used to blend the solution.

Preparation of the TAPP-Loaded Liposomes The TAPP-loaded liposomes were prepared by the dry-film dispersion method. Briefly, the SPC (50 mg) and cholesterol (40 mg) was dissolved in 15 mL chloroform/methanol (1:3 v/v) and rotary evaporated to form a thin film at 37 ℃. After complete removal of the organic solvent, 10 mL of phosphate-buffered solution (pH 7.4) containing 9 mg of TAPP was added to the lipid film as a hydration solution and shaken in a water bath for one hour. The processing temperature was maintained at 37 ℃. The obtained suspensions were sonicated at 800 W (intermittent operation for 10 seconds on and 10 seconds off) for 30 minutes to obtain small and uniform liposome vesicles. Then homogenized by extrusion 100 nm polycarbonate membranes, and purified by passing through a Sephadex G50 gel-filtration column to remove free TAPP.

Characterization of the TAPP-Loaded Liposomes The percentage of encapsulated TAPP was measured in two steps. Firstly, the entrapment efficiency of TAPP-loaded liposomes was determined by G50 gel column method. The obtained liposomes before chromatographic purification were divided into two equal parts. One part was separated by G50 column against phosphate buffers (pH 7.4). The other part was diluted into the same volume of the collected sample above. These two samples were then lysed with 0.1% v/v Triton X-100 and released TAPP was detected by ultraviolet spectrophotometer. Entrapment efficiency of the TAPP-loaded liposomes (EE_{TAPP} %) was calculated as:

$EE_{TAPP}\ \% = W/W_0 \times 100$;

where W and W_0 are the TAPP content in purified liposomes and total amount in dispersion, respectively.

Percent TAPP loading of the prepared liposomes (PDL_{TAPP} %) was calculated as:

$PDL_{TAPP}\ \% = W/(W+W_e) \times 100$;

where W is the TAPP content in purified liposomes and W_e is the total amount of excipients.

Synthesis and Purification of the GO sheets The GO was synthesized from natural graphite powder by modified Hummer's method[19, 20]. In detail, graphite powder (3.0g) was put into an 80 °C solution of concentrated H_2SO_4 (12.0 ml) containing P_2O_5 (2.5g), and $K_2S_2O_8$ (2.5g) for 4.5 h. The mixture was cooled to room temperature, filtered and washed with water using a 0.45 μm microporous membrane. Subsequently, these pre-oxidized graphite powder were put into cold (0 °C) concentrated H_2SO_4 (120.0 ml). Then, $KMnO_4$ (15.0g) was slowly added under stirring. Successively, the mixture was stirred at 35 °C for 2 h and then diluted with water (250 ml) in an ice-bath to keep the temperature below 50 °C. The mixture was stirred for 2 h, and then filtered, washed and dried. Finally, it was purified by dialysis for one week to remove the remaining metal species.

Detection of the PLA_2 and the α-toxin Aliquots (425 μL) of pH 7.4 PBS buffer containing 0.5 mM $CaCl_2$ and different concentrations of the PLA_2 (0-50 nM) or the α-toxin (0-500 nM) were at first maintained in the 1.5-ml vial. Then 50 μl of the TAPP-loaded liposomes were added and the resulting mixture was incubated for different time at 37 °C. Subsequently, 25 μl of the 0.2 mg ml^{-1} GO was added and vortex-mixed thoroughly. The solution was then incubated for another 5 min at ambient temperature and rapidly used for the fluorescence detection.

Inhibitor assay of the PLA_2 and the α-toxin For the inhibitor assay, various concentrations of the chlorpromazine (0.5-100 μM) or the baicalin (2.2-107.5 μM) were firstly incubated with the PLA_2 (9.6 nM) or the α-toxin (289.2 nM) and the TAPP-loaded liposome in 475 μL of pH 7.4 PBS buffer solution at 37 °C for 40 min, respectively. Then 25 μl of the 0.2 mg ml^{-1} GO was added into the solutions, which were incubated for another 5 min at the ambient temperature. Subsequently, the mixtures were rapidly used for the determination of activity of the PLA_2 or the α-toxin on basis of the fluorescence response. All the data analysis is performed with Origin 8.0 software.

Results and discussion

The TAPP-loaded liposomes were purified through a Sephadex G50 gel-filtration column to remove the untrapped TAPP molecules. The nearly spherical shape of liposomes were observed under transmission electron microscopy (Fig. S1a, ESI), and had a narrow size distribution (Fig. S1b, ESI) with an average hydrodynamic radius of 62 ± 7 nm and a slightly negative zeta potential (ζ) of -8.7 ± 1.3 mv, which is in good agreement with the result reported previously[10, 21]. The entrapment efficiency of TAPP was 83.5% and the percentage loading was 7.6%, and for a total lipid concentration of 125 μg ml^{-1}, the concentration of TAPP was about 2.2 μM in the event of 100% release. The atom force microscope image provided solid evidence for the single-layer sheet of the obtained GO (Fig.

S1c, ESI) and the average thickness was measured to be approximately 1.0 nm (Fig.S1d, ESI), which is consistent with the previously reported data [18, 22-23]. It was found that encapsulating the TAPP molecules within the liposomes can high-efficiently obstruct the energy transfer from excited porphyrin to GO sheets. Evidenced by the subsequent fluorescence measurements, addition of GO suspension to the TAPP-loaded liposomes resulted in a negligible change in fluorescence intensity, which indicated that the combination of the TAPP-loaded liposomes and the GO may be potential value in the areas of designing fluorescence assay and inhibitor screening for membrane pore-forming active proteins. Furthermore, the TAPP-loaded liposomes exhibited a good stability and after two weeks of storage at 4 ^{0}C there was no obvious detectable leakage (Fig.S2, ESI).

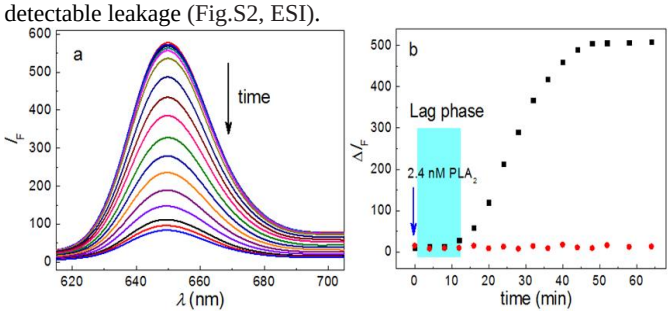

Figure 1 (a) Fluorescence spectra obtained for the TAPP-loaded liposome and graphene oxide plus PLA_2 at different time. (b) Fluorescence response (I_{F0} - I_F, ΔI_F) at 650 nm obtained for the TAPP-loaded liposome and graphene oxide plus PLA_2 in the absence (red) and presence (black) of Ca^{2+}. Concentration: Total lipid concentration, 125 μg ml^{-1}; GO, 8.0 μg ml^{-1}; PLA_2, 2.4 nM.

When exposed to the PLA_2, the degradation of the liposomes resulted in the release of the entrapped TAPP molecules, which caused a significant fluorescence quenching of the TAPP molecules, due to the assembly onto the surfaces of GO sheets to generate energy transfer-based quenching system. As shown in Fig. 1a, the fluorescence signal transduction enabled real-time monitoring of the enzymatic activity. Generally, the catalytic activity of the PLA_2 is highly dependent on the presence of Ca^{2+}, therefore, repeating the experiments in the absence of Ca^{2+} would be useful negative control[24]. As expected, no fluorescence change occurred in the absence of Ca^{2+} upon addition of PLA_2 (red line in Fig. 1b). The results confirm that the fluorescence quenching of the TAPP is dependent on the PLA_2-mediated hydrolysis of the liposomes. A further observation was that the addition of PLA_2 did not give rise to an immediate fluorescence signal change (Fig. 1a and b) but rather showed a typical lag-burst behaviour, which usually ascribed to an accumulation of hydrolysis products in the bilayer, especially fatty acids [10, 25].

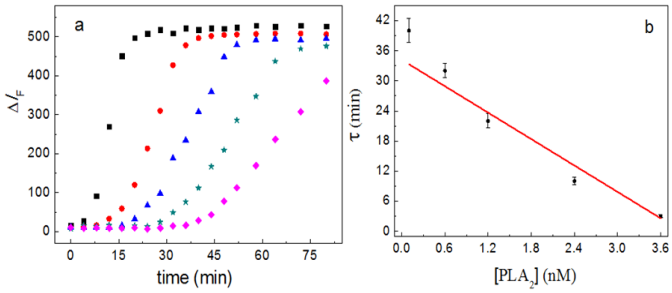

Figure 2 (a) Fluorescence response (ΔI_F) for 9.6 nM, 2.4 nM, 1.2 nM, 600 pM, 200 pM PLA_2 from curve 1 to 5 at 37 ^{0}C. (b) Length of the lag time (τ) as a function of PLA_2 concentration. Concentration: Total lipid concentration, 125 μg ml^{-1}; GO, 8.0 μg ml^{-1}.

As an important kinetic parameter, the duration of the lag phase generally depends upon the concentration and activity of PLA_2 in the sample. With this in mind, a detailed investigation was followed to determine whether the lag time could be used as an appropriate assay metric. As shown in Fig. 2a, the length of the lag time was found to be clearly dependent on the concentration of PLA_2, and spanned from 4 to 45 min for concentrations ranging from 9.6 nM to 200 pM in the presence of 0.5 mM Ca^{2+} at 37 ^{0}C. From the plot of the lag time against the log concentration of PLA_2, a more straightforward linear response can be obtained as the equation of τ = 20.6 - 18.2 *log* [PLA_2] (nM) as shown in Fig. 2b, and the correlation coefficient is 0.9421 with the detection limit (3σ) of 160 pM.

Further, it was found that the temperature and the addition of human serum albumin (HSA) had a significant effect on the length of lag phase, which can be utilized to tune the dynamic range of the assay. For example, at a concentration of 2.4 nM PLA_2, the lag period was about 25 min longer at room temperature than it was at 37 ^{0}C (Fig. S3a, ESI). Similarly, by the introduction of HSA into the TAPP-loaded liposomes, the assay response was significantly enhanced as compared to the same conditions without HSA (Fig.S3b, ESI). However, the HSA alone did not cause any release of the TAPP molecules. The increased release rate of entrapped TAPP by the addition of HSA may be ascribed to their binding sites capable of hosting fatty acid[26], and therefore they can remove the fatty acids accumulated in the membrane, destabilizing the liposomes and resulting in a more rapid hydrolysis.

As described ahead, the α-toxin secreted by *S. aureus* bacteria, one of the most commonly toxin, is another kind of pore-forming protein in artificial or biological membranes[27]. Prior to seeing the α-toxin, the TAPP-loaded liposomes display the strong fluorescence signal even in the presence of GO (curve 1, 2 in Fig. 3a), due to the separation of chromophores from GO sheets, which are protected inside the liposomes and will not be released. However, once the α-toxin encountering the liposomes, they will insert into the membrane to form pores, though which the TAPP molecules can be released from the liposomes. Thus, a significant fluorescence quenching occurred (curve 3 in Fig. 3a), which was consistent with the result of positive control (curve 4 in Fig. 3a) that resulted from the membrane pore-forming surfactant of the 1% Triton X-100.

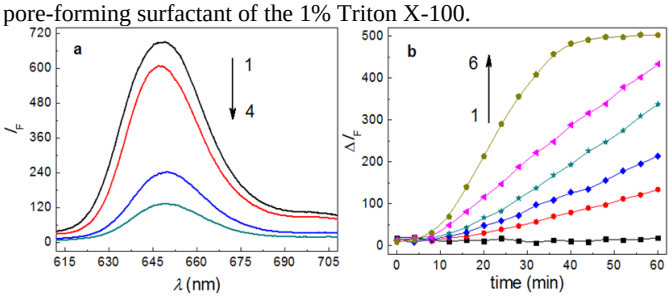

Figure 3 (a) Fluorescence spectra obtained for TAPP-loaded liposome, TAPP-loaded liposome and graphene oxide, TAPP-loaded liposome and graphene oxide plus α-toxin, TAPP-loaded liposome and graphene oxide plus 1% Triton X-100 from curve 1 to 4, respectively. (b) Fluorescence response (ΔI_F) for 0.0 nM, 9.0 nM, 36.0 nM, 72.3 nM, 144.6 nM, 289.2 nM α-toxin from curve 1 to 6 at 37 ^{0}C. Concentration: Total lipid concentration, 125 μg ml^{-1}; GO, 8.0 μg ml^{-1}.

The more detailed investigation on the toxin-triggered TAPP release from the liposome was performed, and it was found that the TAPP release rate is dynamic and dependent on the concentration of the α-toxin. However, compared with the time curves of the PLA_2-mediated TAPP-loaded liposome hydrolysis (Fig. 2a), that of the toxin-triggered TAPP release from the liposomes display different traits. That is, in spite of showing a typical lag phase, the length of the lag time was found not to be dependent on the concentration of α-toxin as shown in Fig. 3b, which may be ascribed to completely different pore-forming mechanism in membranes. We guess that for the α-toxin the length of the lag time could be mainly decided to the rate that the monomer of α-toxin oligomerizes to form a membrane-

inserted heptamer. A further observation is that the fluorescence enhancement (ΔI_F, I_0 - $I_{\alpha\text{-toxin}}$, in which I_0 and $I_{\alpha\text{-toxin}}$ represent the fluorescence emission intensity at 648 nm of the liposome formulations in the absence and presence of different concentrations of α-toxin, respectively), obviously gets increased with the prolonging time. Furthermore, the slope of time curve at the initial stage increases with increasing of the toxin concentration, in other words, the toxin with a higher concentration forms more transmembrane pores and gives rise to a faster initial TAPP release rate. When the toxin is 289.2 nM, it has been found that the ΔI_F do not change any more after 40 min, indicating that the toxin-mediated TAPP release is nearly completed. The obvious fluorescence signal changes clearly demonstrate that the combination of the TAPP-loaded liposome and the GO can be employed as a platform for sensitive monitoring the toxin-mediated release. Thus, a nearly linear plot of ΔI_F versus the α-toxin concentration (c) is obtained (Fig. S4, ESI) and the linear relationship of $\Delta I_F = 1.5\ c + 68.7$ is found in the range of 9.0-289.2 nM with $R = 0.9867$ and a detection limit of 4.8 nM.

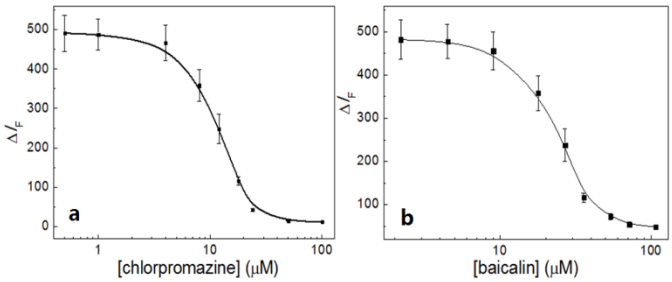

Figure 4 The plot of ΔI_F against the log concentration of inhibitor displaying that the dose-dependent inhibition of the PLA_2 and the α-toxin by the chlorpromazine and the baicalin, respectively. Concentration: Total lipid concentration, 125 μg ml^{-1}; GO, 8.0 μg ml^{-1}; PLA_2, 9.6 nM; α-toxin, 289.2 nM. Incubation time, 40 min.

In general, any biological active protein has its corresponding inhibitor and the activity can be prohibited at a certain degree when the potential inhibitor is present. Therefore, this simple, highly sensitive and convenient fluorescent assay for membrane pore-forming protein could also be employed for the potential inhibitor screening. By taking chlorpromazine as an example, which is a prototypical, water-soluble small molecule inhibitor of PLA_2[13], we firstly incubated the TAPP-loaded liposome with the 9.6 nM of PLA_2 in the presence of chlorpromazine over the range of 0.5-100 μM at 37 °C for 40 min. As shown in Fig. 4a, from the plot of ΔI_F against the log concentration of chlorpromazine, we determined the IC_{50} value of chlorpromazine toward the PLA_2 (9.6 nM) to be 12.0 ± 0.62 μM, which agrees with that reported previously[28].

Baicalin, a flavonoid compound isolated from *Scutellaria baicalensis* Georgi (Huang Qin), is a traditional Chinese medicinal herb. It has also been demonstrated that the baicalin inhibits the hemolytic activity of the α-toxin by influencing the self-assembly and heptamer formation[29]. Similarly, we firstly incubated the TAPP-loaded liposome with the α-toxin in the presence of baicalin over the range of 2.2-107.5 μM at 37 °C for 40 min. From the plot of ΔI_F against the log concentration of the baicalin as shown in Fig. 4b, we can calculate the IC_{50} value of baicalin toward the α-toxin (289.2 nM) to be 26.9 ± 2.6 μM. These results suggest that the combination of the TAPP-loaded liposomes and the GO has a high potential for screening inhibitors of membrane pore-forming active species.

Conclusions

In summary, we have demonstrated a highly sensitive membrane pore-forming protein assay utilizing the GO and the TAPP-loaded liposomes. Using this strategy, we can detect the PLA_2 and the α-toxin concentrations as low as 200 pM and 9.0 nM, respectively. Meaningfully, in addition to determining the levels of the PLA_2 and the α-toxin, we have also verified that this assay could be used to identify the respective inhibitors. We expect that this simple and convenient system will have applications in both other membrane pore-forming protein testing and research-level high throughput inhibitor screening of potential drug candidates.

All authors herein greatly appreciate the financial supports from the National Natural Science Foundation of China (NSFC, 21205096), the Fundamental Research Funds for the Central Universities (XDJK2013A015), and the Program for Innovative Research Team in University of Chongqing (2013).

Notes and references

Key Laboratory of Luminescent and Real-Time Analytical Chemistry, Ministry of Education, College of Pharmaceutical Sciences, Southwest University, Chongqing 400715

†To whom all correspondence should be addressed. Tel: 86-23-68251225; E-mail:lzdzhy@swu.edu.cn; chongli2009@gmail.com.

Electronic Supplementary Information (ESI) available: [details of any supplementary information available should be included here]. See DOI: 10.1039/c000000x/

1. E. A. Dennis, *J. Biol. Chem.* **1994**, *269*, 13057-13060.
2. C. M. Ballantyne, R. C. Hoogeveen, H. Bang, J. Coresh, A. R. Folsom, G. Heiss, A. R. Sharrett, *Circulation* **2004**, *109*, 837-842.
3. Y. Shi, P. Zhang, L. Zhang, H. Osman, E. R. Mohler III, C. Macphee, A. Zalewski, A. Postle, R. L. Wilensky, *Atherosclerosis* **2007**, *191*, 54-62.
4. S. Bhakdi, J. Tranum-Jensen, *Microbiol. Rev.* **1991**, *55*, 733-751.
5. E. Gouaux, *J. Struct. Biol.* **1998**, *121*, 110-122.
6. D. A. Giljohann, C. A. Mirkin, *Nature* **2009**, *462*, 461-464.
7. S. Song, Y. Qin, Y. He, Q. Huang, C. Fan, H.-Y. Chen, *Chem. Soc. Rev.* **2010**, *39*, 4234-4243.
8. T. M. Rose, G. D. Prestwich, *ACS Chem. Biol.* **2006**, *1*, 83-92.
9. S. Chemburu, E. Ji, Y. Casana, Y. Wu, T. Buranda, K. S. Schanze, G. P. Lopez, D. G. Whitten, *J. Phys. Chem. B* **2008**, *112*, 14492-14499.
10. D. Aili, M. Mager, D. Roche, M. Stevens, *Nano Lett.* **2011**, *11*, 1401-1405.
11. S. J. Liu, Q. Wen, L. J. Tang, J. H. Jiang, *Anal. Chem.* **2012**, *84*, 5944-5950.
12. W. Y. Chen, L. Y. Chen, C. M. Qu, C. C. Huang, S. C. Wei, H. T. Chang, *Anal. Chem.* **2013**, *85*, 8834-8840.
13. Y. F. Xu, Z. B. Liu, X. L. Zhang, Y. Wang, J. G. Tian, Y. Huang, Y. F. Ma, X. Y. Zhang, Y. S. Chen, *Adv. Mater.* **2009**, *21*, 1275-1279.
14. Y. X. Xu, L. Zhao, H. Bai, W. J. Hong, C. Li, G. Q. Shi, *J. Am. Chem. Soc.* **2009**, *131*, 13490-13497.
15. A. Wojcik, P. V. Kamat, *ACS Nano* **2010**, *4*, 6697–6706.
16. J. X. Geng, H. T. Jung, *J. Phys. Chem. C* **2010**, *114*, 8227-8234.
17. H. Hayashi, I. V. Lightcap, M. Tsujimoto, M. Takano, T. Umeyama, P. V. Kamat, H. Imahori, *J. Am. Chem. Soc.* **2011**, *133*, 7684-7687.
18. Z. D. Liu, H. X. Zhao, C. Z. Huang, *Plos One*, **2012**, *7*, e50367.
19. W. S. Hummers, R. E. Offeman, *J. Am. Chem. Soc.* **1958**, *80*, 1339-1939.
20. Y. Xu, H. Bai, G. Lu, C. Li, G. Shi, *J. Am. Chem. Soc.* **2008**, *130*, 5856-5857.
21. A. Kunze, S. Svedhem, B. Kasemo, *Langmuir* 2009, *25*, 5146-5158.
22. H. C. Schniepp, J. L. Li, M. J. McAllister, H. Sai, M. Herrera-Alonso, D. H. Adamson, R. K. Prud'homme, R. Car, D. A. Saville, I. A. Aksay, *J. Phys. Chem. B* **2006**, *110*, 8535-8539.
23. D. Li, M. B. Muller, S. Gilje, R. B. Kaner, G. G. Wallace, *Nat. Nanotechnol.* **2008**, *3*, 101-105.
24. E. A. Dennis, *J. Biol. Chem.* **1994**, *269*, 13057-13060.
25. W. R. Burack, R. L. Biltonen, *Chem. Phys. Lipids* **1994**, *73*, 209-222.
26. A. A. Bhattacharya, T. Greune, S. Curry, *J. Mol. Biol.* **2000**, *303*, 721-732.
27. D. Pornpattananangkul, L. Zhang, S. Olson, S. Aryal, M. Obonyo, K. Vecchio, C. M. Huang, L. Zhang, *J. Am. Chem. Soc.* **2011**, *133*, 4132-4139.
28. M. Lindahl, C. Tagesson, *Inflammation* **1993**, *17*, 573-582.

29. J. Qiu, X. Niu, J. Dong, D. Wang, J. Wang, H. Li, M. Luo, S. Li, H. Feng, X. Deng, *J. Infect. Dis.* **2012**, *206*, 292-301.